Journal of Renewable Materials

Tech Science Press

DOI: 10.32604/jrm.2021.015793

ARTICLE

Different Effects of Wet and Dry Grinding on the Activation of Iron Ore Tailings

Yingchun Yang[1,*], Liqing Chen[1] and Yuguang Mao[2]

[1]College of Engineering, Anhui Agricultural University, Hefei, 230036, China

[2]College of Civil Engineering, Hunan University, Changsha, 410082, China

*Corresponding Author: Yingchun Yang. Email: yangyingchun1983@163.com

Received: 14 January 2021 Accepted: 09 March 2021

ABSTRACT

Improving the activity of Iron Ore Tailings (IOTs) to utilize them as a mineral admixture in cement-based minerals is still challenging. In this paper, the wet grinding technology was employed to stimulate the activity of IOTs, and the traditional dry grinding method was used as a reference. The effect of wet grinding on the activation of IOTs was evaluated through ion leaching from an alkaline solution and the reactivity index. Additionally, a detailed comparison between Dry-grinding Iron Ore Tailings (DIOTs) and Wet-grinding Iron Ore Tailings (WIOTs) was made. This comparison was based on particle characteristics, crystal structures, chemical structure, and surface properties. The results showed that the particle size of IOTs reduced rapidly during wet grinding. In addition, WIOTs had a higher activity index compared to DIOTs. The storage of lattice distortions in the quartz crystal structure was also more significant during the wet grinding process than during the dry grinding process. Moreover, both prolonged dry and wet grinding could destabilize the Si-O bond and decrease the surface binding energy.

KEYWORDS

Wet grinding; iron ore tailings; particle characteristics; mineral admixture

1 Introduction

Iron Ore Tailings (IOTs) refer to the solid waste associated with the process of iron concentrate extraction from iron ore and are an important source of environmental pollution [1,2]. Approximately 5 billion tons of IOTs are currently present in China, and more than 600 million tons are produced every year. Given that the utilization rate of IOTs is less than 10% [3,4], such large amounts not only occupy excessive space but also present a significant hazard to human health and the environment [5]. Therefore, comprehensive utilization of IOTs has been the focus of most studies in an effort to minimize environmental pollution and achieve sustainable development [6–8].

The major chemical components of IOTs are similar to those of cement and include SiO_2, Al_2O_3, CaO and Fe_2O_3 [9]. Therefore, IOTs are widely used to prepare building materials such as concrete fine aggregates [10–12], autoclaved aerated concrete [13–15], building ceramics [16–18] and wall material [19–22]. Currently, IOTs are ground into fine powder in order to improve the efficiency of ore dressing. In actual fact, using IOTs for the preparation of supplementary cementitious materials is considered more feasible [23–25]. However, IOTs show a very low activity compared to common mineral admixtures such as fly ash, silica fume, and ground blast-furnace slag [23]. Therefore, improving the activity is considered

important to promoting the recyclability of IOTs in building materials. Typical methods for improving the activity of IOTs mainly involve mechanical grinding [26,27] as well as chemical and thermal activation [28–30]. Compared to the other two methods, mechanical grinding has the advantage of being a relatively simple activation process that does not require chemical activators and is environmentally friendly [31,32]. Additionally, mechanical grinding can not only decrease the particle size of IOTs but also induce changes in crystal structures [23]. However, in order to achieve more fineness, several hours of dry-milling are required, and this leads to high consumption of energy [33]. Moreover, Kumar et al. [34] showed that particle agglomeration might occur after a long time of dry-grinding. Therefore, it is essential to search for high efficiency and low energy consumption techniques that improve the activity of IOTs.

Wet grinding refers to the pulverization of solid powder under water-based conditions and is different from the traditional mechanical crushing technique. Due to the presence of a water medium, a series of physical and chemical changes take place in the mineral admixtures during grinding and placing [33]. Tan et al. [35] showed that wet grinding could significantly reduce the particle size of lithium slag and accelerate the dissolution of lithium, aluminum, and silicon. Yang et al. [33] found that the pozzolanic reactivity of fly ash was greatly improved after wet grinding and confirmed that the activation mechanism of wet grinding could achieve physical breakage and acceleration of ion dissolution. Wang et al. [36] studied the effect of wet grinding on the hydration properties of Blast Furnace Slag (BFS) and found that the technique could dramatically decrease the particle size of BFS and improve its reactivity. Kotake et al. [37] also reported that the wet-milling technology was able to improve the grinding limit of quartz and avoid particle agglomeration. At present, wet grinding technology is mainly used in mineral processing pretreatment, ceramic industry, papermaking industry, and other fields [33]. However, few studies are about using wet grinding technology to stimulate the potential activity of IOTs and applying Wet-grinding Iron Ore Tailings (WIOTs) in cement-based materials. Therefore, the present study investigated the effect of the wet grinding activation technology on the activity of IOTs, and the traditional dry grinding activation technology was used as a reference. Additionally, differences between WIOTs and Dry-grinding Iron Ore Tailings (DIOTs) with regard to physical and chemical structures were studied. Finally, the advantages of WIOTs as a mineral admixture of cement-based materials were discussed.

2 Materials and Methods

2.1 Materials

The cement used in the present study was ordinary Portland cement (P.O 42.5) with a specific surface area of 352 m^2/kg. The IOTs were directly obtained from the beneficiation processing of a mining enterprise in Huoqiu County of Anhui Province. The X-ray diffraction pattern of IOTs is presented in Fig. 1, which shows that the main mineral phase in Raw Iron Ore Tailings (RIOTs) is quartz. The chemical composition of the cement and IOTs performed by X-ray fluorescence are presented in Tab. 1. ISO standard sand (according to GSB08-1337) was used in preparing the mortar samples.

2.2 Preparation of IOTs

DIOTs and WIOTs were prepared in a planetary ball mill with four grinding pots. Each grinding pot included four specification spherical agate balls, with a weight ratio of 10 mm: 8 mm: 5 mm: 3 mm = 1: 3: 6: 2. The total weight of the agate balls in each grinding pot was about 35 g.

Preparation of DIOTs: 20 g IOTs was weighed and put into the grinding pot then milled for 30 min (or 60 min) at a motor speed of 600 r/m. Following this, DIOTs30 (or DIOTs60) were obtained.

Preparation of WIOTs: IOTs (20 g) and water (9 g) were separately weighed and put into the grinding pot. The mixture was then milled for 30 min (or 60 min) at a motor speed of 600 r/m. Thereafter, the agate balls were separated, and WIOTs30 (or WIOTs60) were obtained.

All samples were dried in an oven at 50°C for 24 h before the subsequent experiments.

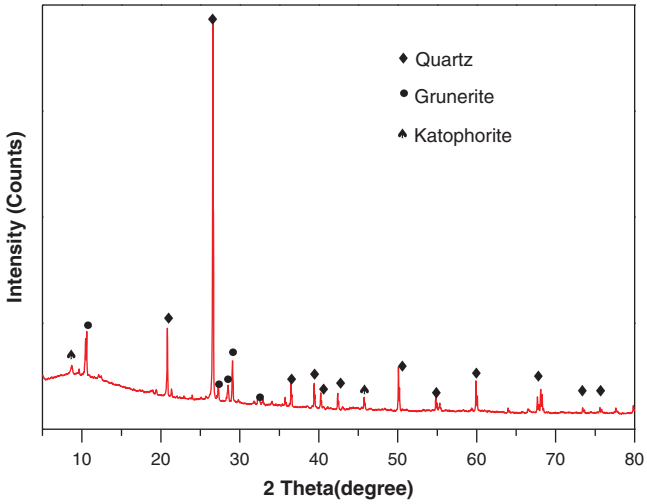

Figure 1: XRD pattern of RIOTs

Table 1: Chemical compositions (by mass) of cement and RIOTs (%)

Raw material	SiO_2	Al_2O_3	Fe_2O_3	CaO	MgO	SO_3	K_2O	Na_2O
cement	21.18	4.09	3.45	61.50	1.16	3.03	1.21	0.24
RIOTs	50.26	4.22	24.36	4.19	14.44	0.34	0.73	0.55

2.3 Methods

The particle size distributions of IOTs were measured by Malvern Mastersizer 2000 (accessory name: Hydro 2000SM). The specific surface area (S) of IOTs was calculated by the following equation: $S = 6/(\rho.D\ [3,2])$ [38], where ρ is the specific mass of IOTs (2.85 g/cm^3) and D [32] is the surface weighted mean.

The morphology of IOTs was observed through the Hitachi S3400 cold field-emission scanning electron microscopy. Additionally, cement and IOTs were mixed at a proportion of 1:1 and stirred evenly in order to study the nucleation effect of IOTs. After 4 h, about 1 g of sample was obtained and dehydrated using anhydrous ethanol. After vacuum drying, the surface of IOTs was observed through Scanning Electron Microscope (SEM).

Inductively coupled plasma spectrometer (ICP) analysis: RIOTs (1 g), DIOTs60 (1 g) and WIOTs60 (1 g) were separately weighed and added into 100 ml of NaOH solution (1.0 mol/L, 2.0 mol/L) respectively. The solution was then incubated at 20°C for 7 d before being filtered. Afterwards, the filtrate was neutralized with 100 ml HCL (1.0 mol/L, 2.0 mol/L) and the solubility of silicon and aluminum ions determined using the ICAP 6300 spectrometer.

The activity index of IOTs was evaluated according to GB/T 12957–2005. The mix proportions of the mortar samples are shown in Tab. 2. The compressive strength of the standard cured specimens was tested at 3 d, 7 d, and 28 d. Additionally, the activity indices for DIOTs30, DIOTs60, WIOTs30, and WIOTs60 were calculated using the ratio of the strength of D30, D60, W30, and W60 to the strength of C0, respectively.

The crystalline phases of RIOTs, DIOTs and WIOTs were characterized by XRD using Cu Kα radiation at 45 kV and 200 mA. A range of 5°–80° and a step size of 0.02° were used. The effect of wet-grinding on the crystalline structure of IOTs was investigated using IR. The IR spectra were recorded on a Nicolette

iS50 infrared spectrometer (Thermo Fisher USA), using the Attenuated Total Reflectance (ATR) with the frequency range of 4000 cm^{-1}–400 cm^{-1}. X-ray Photoelectron Spectroscopy (XPS) was collected with a Thermofisher K-Alpha spectrometer using a monochromatic Al Kα X-ray. The spectra were recorded in the constant analyzer energy scanning mode with pass energy of 100 eV for survey spectra and pass energy of 50 eV for high resolution spectra. High resolution spectra were recorded with a step size of 0.05 eV repeated five times to obtain the elemental and chemical composition of IOTs. High resolution analyses for Si2p, Al2p, and O1s were calibrated to C1s signal of 284.8 eV.

Table 2: The mix proportion of mortars

Sample	Cement/g	DIOTs30/g	WIOTs30/g	DIOTs60/g	WIOTs60/g	Standard sand/g	Water/ml
C0	450	0	0	0	0	1350	225
D30	315	135	0	0	0	1350	225
W30	315	0	135	0	0	1350	225
D60	315	0	0	135	0	1350	225
W60	315	0	0	0	135	1350	225

3 Results

3.1 Particle Size Distributions and Morphology

The characteristic parameters of the RIOTs, DIOTs and WIOTs particles are shown in Fig. 2a. After dry grinding for 30 min, the d (0.1), d (0.5), and d (0.9) values for the IOTs particle group reduced from 19.375, 80.498 and 243.706 μm to 2.041, 22.793 and 66.979 μm, respectively. On the other hand, the values dramatically reduced to 1.578, 8.334, and 18.055 μm respectively after wet-grinding for 30 min. Moreover, from 30 min to 60 min, the d (0.5) of DIOTs slightly reduced from 22.793 μm to 22.738 μm, although there was a continuous decrease in particle size during the wet milling process. Notably, the d (0.5) of WIOTs further reduced from 8.334 μm to 6.203 μm. These indicated that wet grinding was significantly more efficient in pulverizing the IOTs.

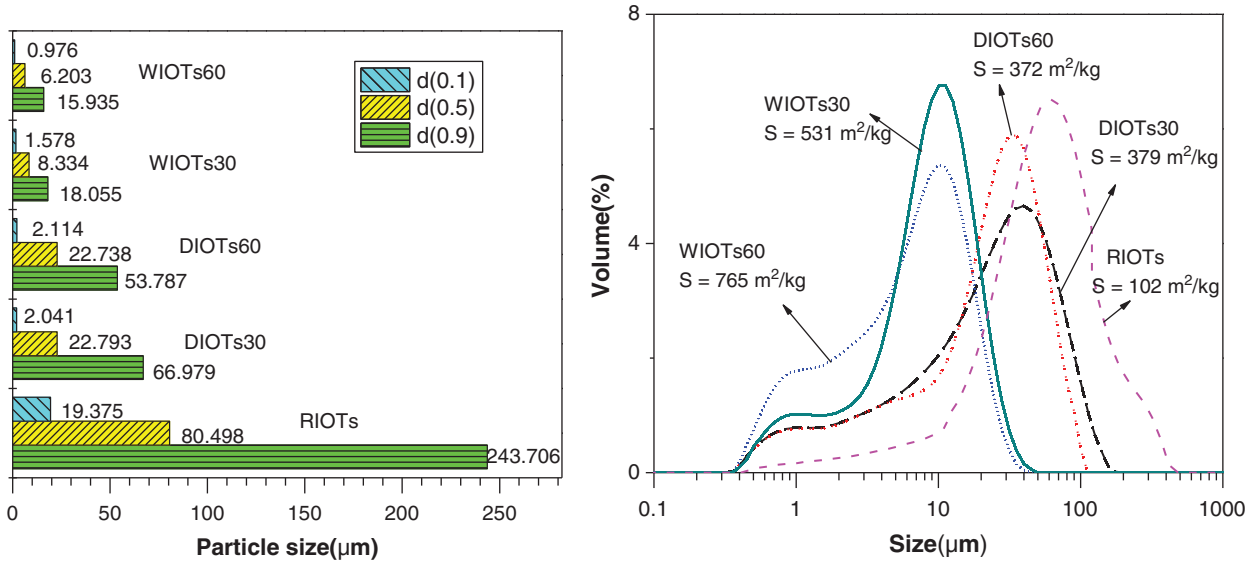

Figure 2: Characteristic particle parameters (a) and particle size distribution (b) of RIOTs, DIOTs and WIOTs

Particle size distribution and the specific surfaces of RIOTs, DIOTs and WIOTs are shown in Fig. 2b. It is worth noting that the specific surface of DIOTs60 was 372 m^2/kg and it was smaller than that of DIOTs30 (379 m^2/kg). This means that particle agglomeration began after 60 minutes of dry grinding. In contrast, the specific surface of WIOTs increased from 531 m^2/kg to 765 m^2/kg between 30 min and 60 min. In addition, the particle width of WIOTs was narrower than that of DIOTs since the particle size ratio d(0.9)/d(0.1) of DIOTs60 was 26.38 while that of WIOTs60 was 16.32. Given that the width of the particles can describe the uniformity of the powder, the results indicated that the WIOTs particles were more uniform than those of DIOTs.

The above results indicated that wet grinding was more conducive to the refinement of IOTs particles than dry grinding. The reasons are mainly related to the interactions between water molecules and the broken surface bonds. It was reported that the agglomeration of particles was easy to occur in the traditional dry grinding process due to the existence of high energy state and electric charge on the surface of broken particles [38], which limit the further reduction of the particle size of IOTs. On the contrary, during the wet grinding process, the water could act as the dispersing medium [33], thus restraining the agglomeration and improving the grinding efficiency. In addition, the existence of a water medium has a buffer effect on the settlement of coarse particles [39], which also leads to the faster crushing and refinement of coarse particles in the wet grinding process.

The uniform distribution and refinement of IOTs particles are also highlighted by the morphological images in Fig. 3. SEM micrographs showed that RIOTs had large particles, a rough surface, and an irregular shape. In addition, some small particles could be seen adhering to the surface of the large ones. After dry grinding for 60 min, the large particles were broken, and the particle size remarkably decreased. Moreover, some of the DIOTs60 small particles assumed a rod-like morphology with a diameter of 2 μm and a length of 20 μm, as shown in Fig. 3b.

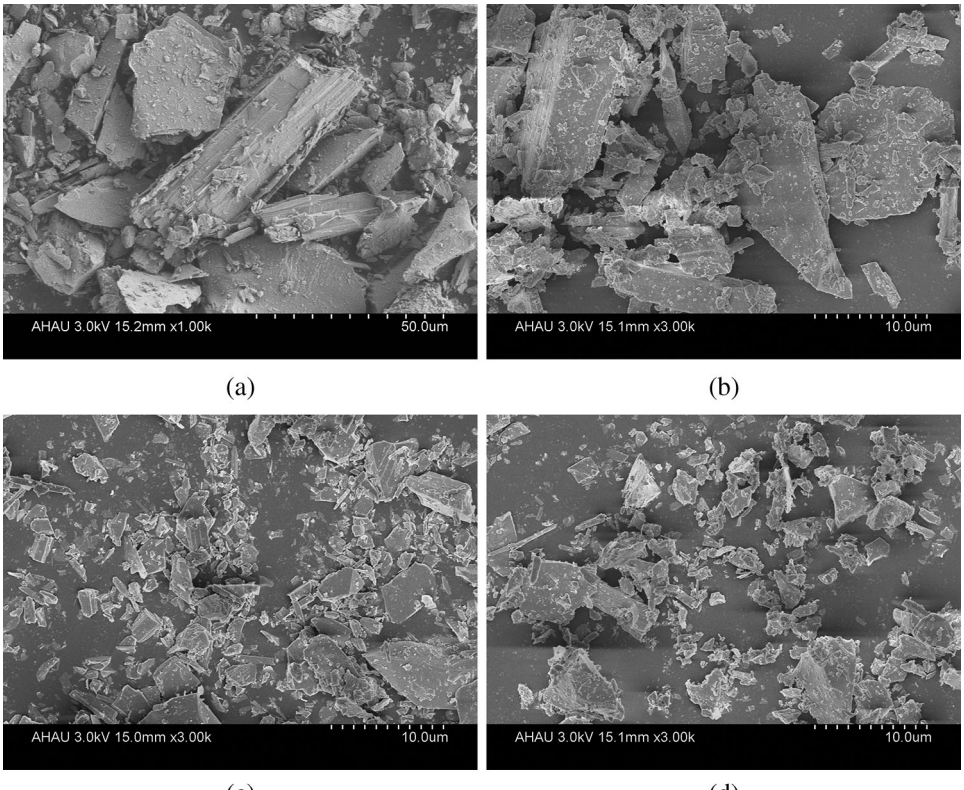

Figure 3: SEM images of IOTs. (a) RIOTs; (b) DIOTs60; (c) WIOTs30 (d) WIOTs60

The particle size of WIOTs was significantly smaller than that of DIOTs60. In addition, all of the large particles were broken after 30 min of wet grinding, and a large number of submicron particles could be seen, as shown in Fig. 3c. Moreover, smaller IOTs particles that were uniformly distributed appeared after 60 min of wet grinding (Fig. 3d), consistent with the results of particle size analysis. Notably, the morphology of WIOTs60 was still irregular, and there was no significant difference in the surfaces of DIOTs60 and WIOTs60.

3.2 Leaching Behavior and Reactivity Index

In this study, the leaching behavior of ions and the strength activity index were used to evaluate the activity of WIOTs. Generally, the activity of a mineral admixture mainly depends on the amount of activated silicon and aluminum, capable of reacting with the $Ca(OH)_2$ produced from cement hydration. Therefore, this is a direct and quick method of evaluating the activity of mineral admixtures and is based on the number of active components dissolved in an alkaline solution [40].

In the present study, different concentrations of NaOH (1.0 mol/L, 2.0 mol/L) were prepared for the leaching test. The amount of dissolved silicon and aluminum were measured through ICP, and the results are shown in Fig. 4. It was observed that an increase in the concentration of NaOH led to a corresponding increase in the concentration of dissolved Si+Al in RIOTs, DIOTs, and WIOTs. Furthermore, the concentration of dissolved Si+Al in WIOTs60 was higher than that of DIOTs60 at the same concentration of NaOH, while that of WIOTs30 was higher than that of DIOTs30. It is well known that the higher the concentration of dissolved Si+Al ionic groups in NaOH solutions, the larger their contribution to subsequent reactions in cement-based materials. The results indicated that wet grinding was more effective at stimulating the activity of IOTs compared to dry grinding in the same duration.

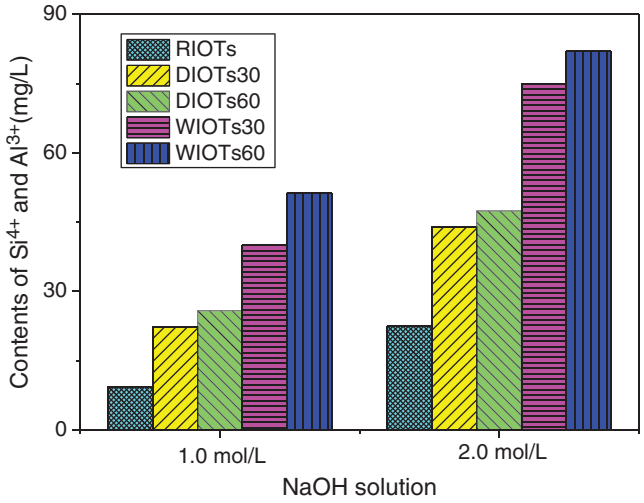

Figure 4: Contents of Si^{4+} and Al^{3+} in NaOH solution dissolved out from IOTs

It is worth noting that the concentration of dissolved Si+Al in WIOTs30 was also higher than that of DIOTs60 at the same concentration of NaOH. This meant that wet grinding was indeed more efficient in stimulating the activity of IOTs compared with dry grinding. Besides, it was also observed that the concentration of dissolved Si+Al in DIOTs60 was higher than that of DIOTs30, and that of WIOTs60 was higher than that of WIOTs30 at the same concentration of NaOH. It indicated that whether DIOTs or WIOTs, the longer grinding time, the higher the activity.

In addition, compressive strength is used as an indirect indicator of activity. The strengths of mortars containing IOTs compared to those with pure cement are presented in Fig. 5. It can be seen that the strength of all samples increased with the increase of curing time. Furthermore, mortar W30 had higher compressive strength than mortar D30, and mortar W60 had higher compressive strength than mortar D60 at the same curing time. Moreover, the reactivity index of WIOTs60 was higher than that of DIOTs60, and that of WIOTs30 was higher than that of DIOTs30, as shown in Fig. 6. For instance, at 28 days, the reactivity index of WIOTs60 was 79% and this was greatly higher than that of DIOTs60 at 65%. Likewise, the reactivity index of WIOTs30 was 73%, which was higher than that of DIOTs30 (64%). These results further proved that wet grinding was more conducive to the activation of IOTs compared with dry grinding in the same duration. Besides, it can be noted that the reactivity index of DIOTs60 at 3 d and 7 d was slightly lower than that of DIOTs30, which might be related to the particle characteristics of the two. As shown in Fig. 2, the difference in particle size distribution between DIOTs60 and DIOTs30 was small, while the specific surface of DIOTs30 was slightly higher than that of DIOTs60, therefore, DIOTs30 had a slight advantage in the nucleation inducing effect in the cementing materials at the early age. However, the reactivity index of DIOTs60 at 28 d was higher than that of DIOTs30, which meant that the pozzolanic activity of DIOTs60 was higher than that of DIOTs30. These results indicated that grinding time had a positive effect on the pozzolanic activity of IOTs.

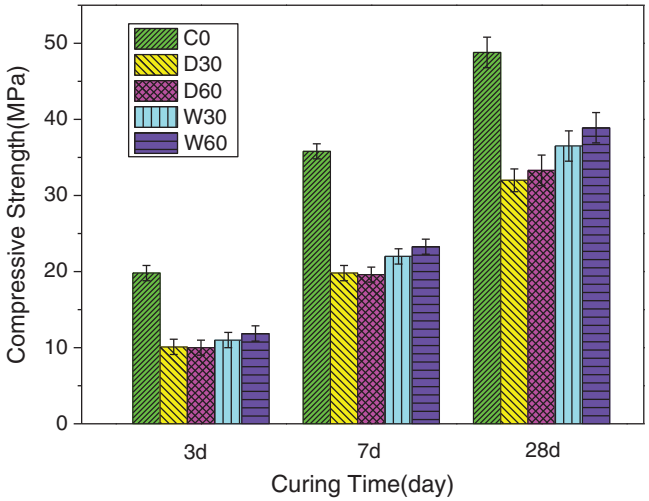

Figure 5: Compressive strengths of IOTs mortars

Based on the above results, both dry and wet grinding could improve the activity of IOTs, and WIOTs were more active than DIOTs at the same grinding time. The increased activity of WIOTs may improve the utilization rate of IOTs in cement-based materials. Moreover, the leaching behavior of ions was related to particle fineness and phase composition. Finally, strength was a comprehensive index of cement mortar, which was related to various factors, including hydration agents, pore characteristics, and microstructure. The study then sought to further understand the mechanisms underlying the effect of wet grinding on the activity of IOTs. Therefore, differences between wet grinding and dry grinding on mechano-chemical activation of IOTs were investigated and discussed in detail in a later section.

3.3 Phase Composition

Fig. 7 shows typical XRD patterns of DIOTs and WIOTs ground at different times. The results showed that the intensity of quartz diffracting peaks decreased with an increase in grinding time. A similar decrease in peak intensity was reported in traditional mechanically activated IOTs [23]. However, it is worth noting that

the decrease in peak intensity of WIOTs was more pronounced than that of DIOTs. The decrease in peak intensity indicates a reduction in crystallinity. Therefore, it is possible that both dry and wet grinding could reduce the crystallinity of IOTs, and wet grinding had a more substantial reducing effect compared to dry grinding. Additionally, the Full-width at Half-maximum (FWHM) of the major quartz diffracting peak was measured in order to evaluate peak line broadening and crystallite size of the IOTs. The FWHM values for RIOTs, DIOTs60 and WIOTs60 were 0.0192°, 0.0279° and 0.0393°, respectively. It is known that the smaller the FWHM, the larger the crystallite size, these results demonstrated that wet grinding could cause a more significant increase in the amorphous phase and crystal lattice deformation of quartz compared to dry grinding.

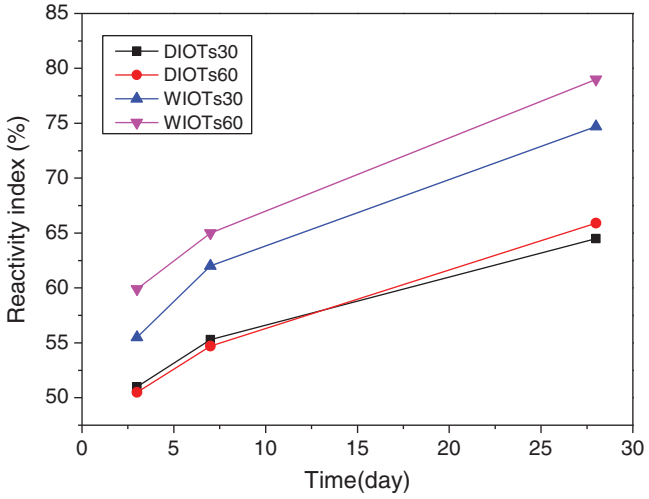

Figure 6: Reactivity indexes of DIOTs and WIOTs

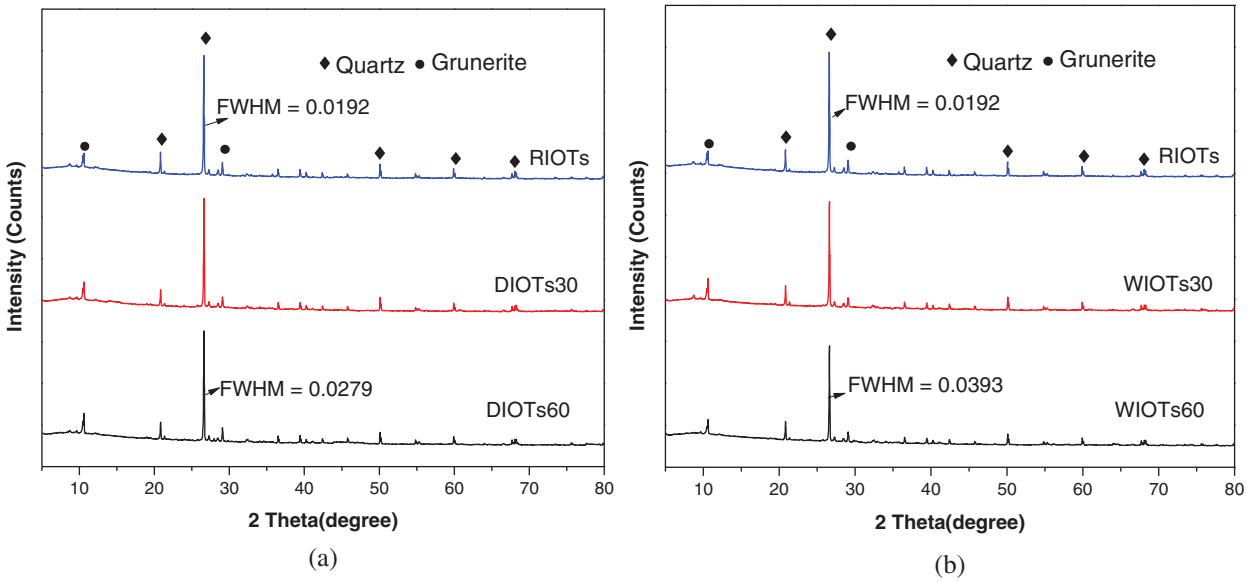

Figure 7: XRD patterns of DIOTs and WIOTs: (a) DIOTs; (b) WIOTs

Fig. 8 shows the local image of the main quartz diffraction peak. The main diffraction peak shifted to a higher 2θ value during the dry and wet grinding processes with prolonged grinding time. Similarly, shifting was more significant during wet grinding compared to dry grinding. Shifting of the diffraction peak might have resulted from crystal lattice distortion and generation of residual stress [8]. Therefore, the results further revealed that wet grinding more likely led to lattice defects in IOTs and activated their potential activity. The reason can be understood from the input energy imparted by the grinding media. According to Guzzo et al. [38], the lattice defects such as point defects and dislocations are caused by the absorption of mechanical energy in the grinding media. As shown in Fig. 2, the particle size of WIOTs60 was significantly smaller than that of DIOTs60, indicating that WIOTs absorbed more mechanical energy than DIOTs with the same grinding time, thus contributing to producing more lattice distortion and defects and improving the amorphous phase. More amorphous phases appearing during wet grinding will help the reaction in cement-based materials, which should be one of the reasons for the higher strength of WIOTs.

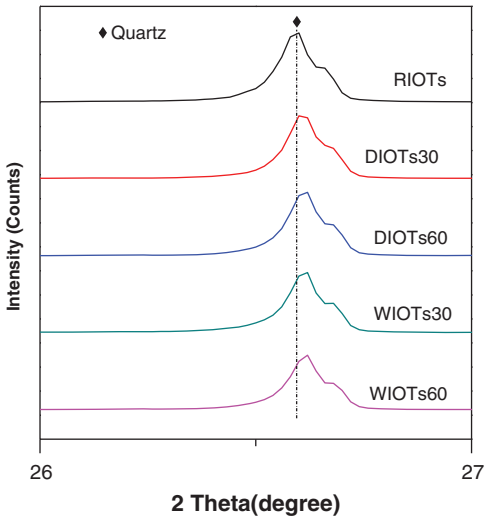

Figure 8: XRD patterns of DIOTs and WIOTs: 26°–27°

3.4 Surface Characteristic

XPS analysis was used to characterize the effects of dry and wet grinding on the surface characteristics of IOTs. The XPS survey spectra (Fig. 9) show that the main surface components of IOTs were oxygen, silicon, aluminum and calcium.

The high-resolution scan curves for Si2p, Al2p, and O1s, which are important for the pozzolanic reaction of IOTs, are shown in Fig. 10. The figure shows that the binding energies of Si2p, Al2p, and O1s were almost constant after 30 min of grinding, although they declined after 60 min in both dry and wet grinding. A short grinding duration was shown to have no effect on the surface characteristics of IOTs. A decrease in binding energy indicates that the coupling of atoms to electrons is weakened, and chemical bonds are more likely to break, further improving the pozzolanic activity of IOTs. Therefore, a long grinding time is necessary to activate the pozzolanic reactivity of IOTs.

It is noteworthy that the decrease in binding energy during the dry grinding process was more pronounced than in wet grinding. This may have been due to differences in the grinding kinetics of the wet and dry methods. It was also reported that the crushing effect of wet grinding was related to the viscosity of the slurry [36]. Moreover, previous reports on the results of particle size analysis showed that the IOTs particle size dramatically decreased during the first 30 min of wet grinding while the viscosity of the slurry increased rapidly. With an increase in slurry viscosity, fine IOTs particles began to deposit on the inner surface of the mill, leading to fewer collisions [39]. The surface of fine particles in WIOTs had little friction due to adhesion, thus interfering with the decrease in surface binding energy.

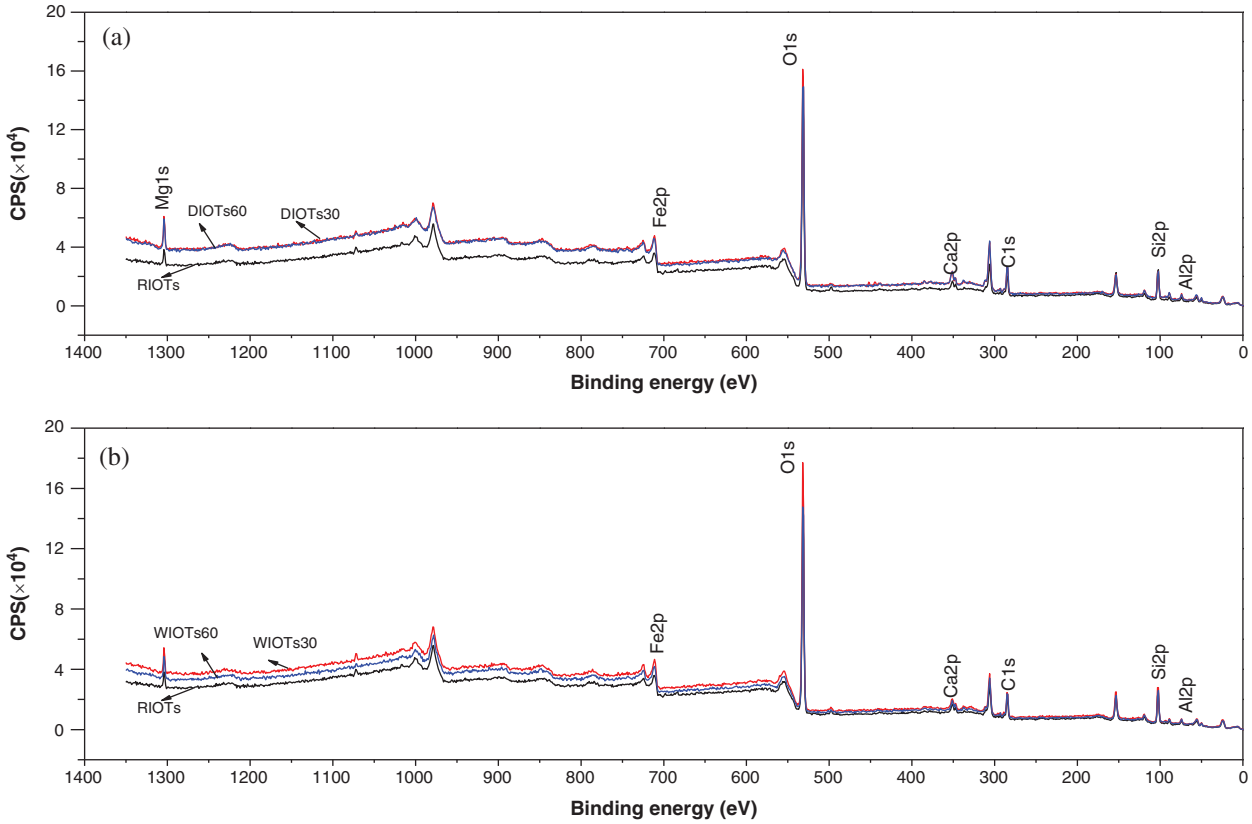

Figure 9: XPS survey spectrums of RIOTs, DIOTs (a) and WIOTs (b)

3.5 Chemical Structure

The IR spectra of RIOTs, DIOTs, and WIOTs are presented in Fig. 11. The figure shows that no new absorption peaks emerged in the IR spectra of DIOTs and WIOTs, compared to that of RIOTs. This suggests that no new functional groups were produced during the dry and wet grinding processes. The peak around 975 cm^{-1} resulted from the asymmetrical stretching vibration of Si-O, while the bending vibration of Si-O appeared at around 441 cm^{-1}. The peaks at 637 cm^{-1}, 695 cm^{-1}, and 774 cm^{-1} can be attributed to the symmetric stretching vibration of Si-O-Si. Additionally, there was a marked increase in absorbance with increasing grinding time. Notably, absorbance in WIOTs was higher than that in DIOTs, and this may be associated with the distribution of IOTs particles. According to Guzzo et al. [38], the efficiency of ATR can be improved if the surface of the crystal analyzer is covered with a layer of compact particles. Therefore, the finer particle size of WIOTs was important for the compactness of the layer.

Furthermore, some changes appeared in the Si-O vibrations at around 441 cm^{-1} and 975 cm^{-1} after grinding. The peak at around 441 cm^{-1} became sharp and began to split after dry and wet grinding. Moreover, with increasing grinding time, there was a decreased shift in frequency of the Si-O band at around 975 cm^{-1} in both the dry and wet processes. Some slight differences were observed between the dry and wet grinding techniques. First, the WIOTs peak splitting at around 441 cm^{-1} was more evident than that of DIOTs. Additionally, the DIOTs peak splitting at around 975 cm^{-1} was a little sharper than that of WIOTs. However, no significant differences were observed in the DIOTs and WIOTs spectra. Both peak splitting and shifting of the Si-O band predicted a decrease in the stability of the Si-O bond. These observations suggested that both dry and wet grinding could destabilize the Si-O bond. Destruction of the stability of Si-O bond would be helpful for the depolymerization and bond breaking during the pozzolanic reaction in cement-based materials.

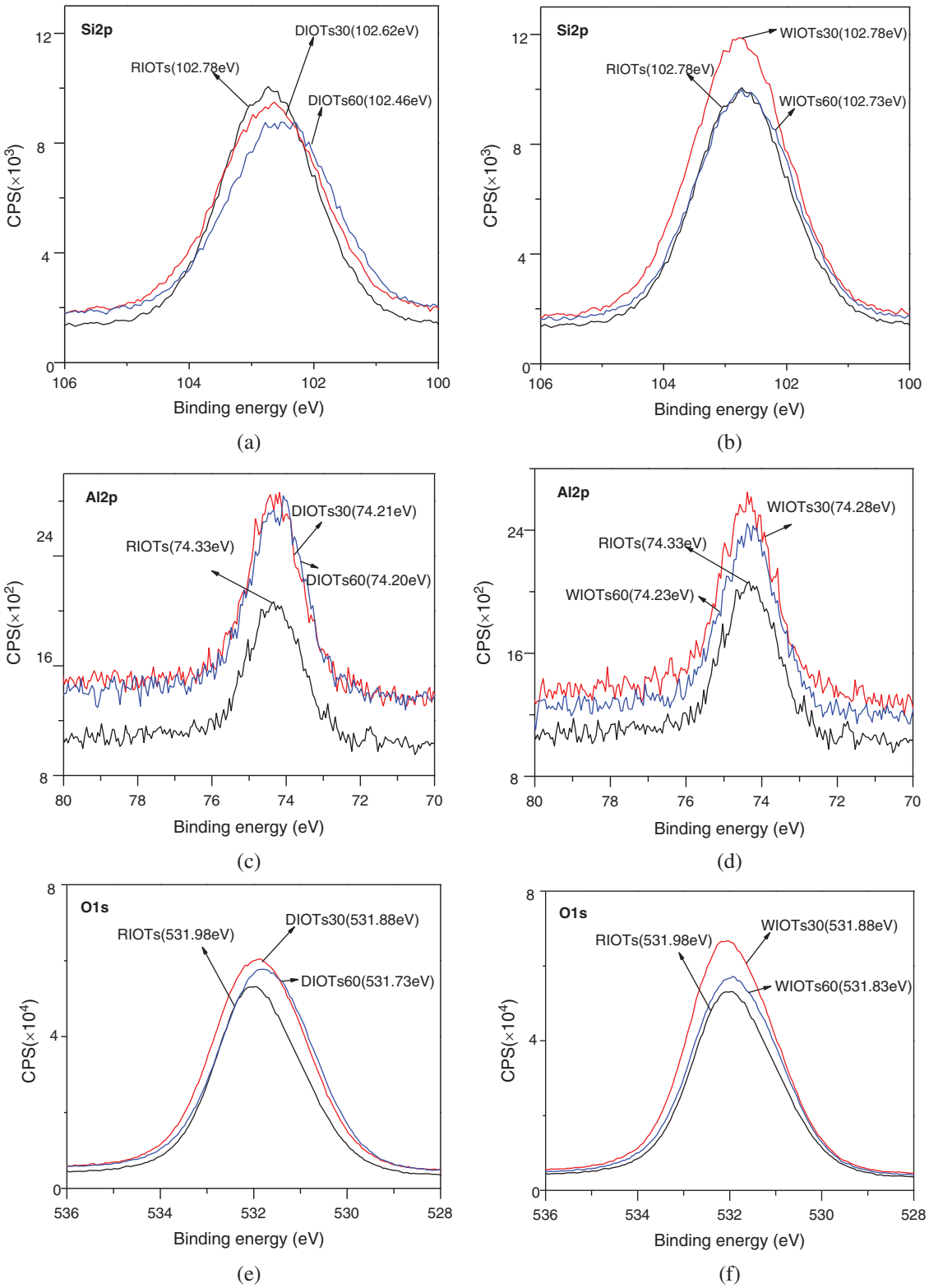

Figure 10: High resolution scan curves of RIOTs, DIOTs and WIOTs. (a) Si2p of DIOTs; (b) Si2p of WIOTs; (c) Al2p of DIOTs; (d) Al2p of WIOTs; (e) O1s of DIOTs; (f) Q1s of WIOTs

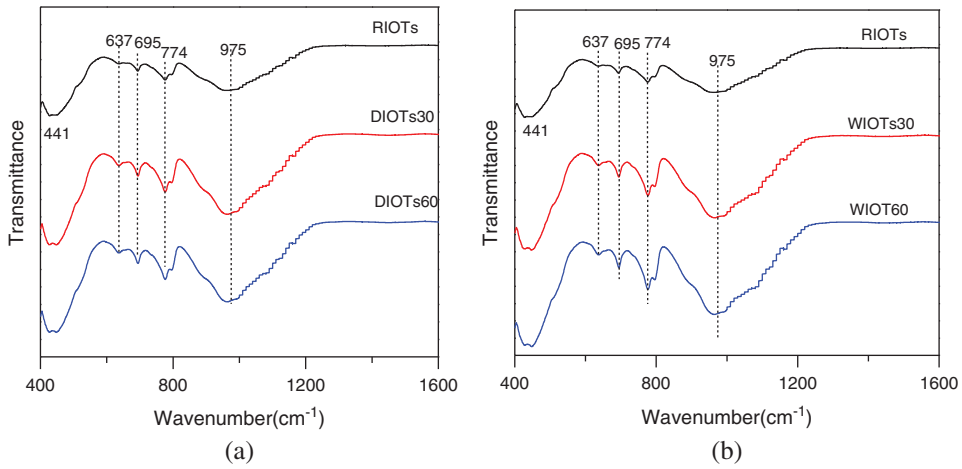

Figure 11: FTIR spectrums of IOTs (a) before and after dry-grinding; (b) before and after wet grinding

4 Discussions

The results showed that both dry and wet grinding could change the physical and chemical properties of IOTs, including particle size, crystal structure, chemical structure, and surface characteristics, thus improving their activity. However, based on the results of leaching behavior and strength reactivity index, WIOTs was shown to have more advantages as the mineral admixture of cement-based materials compared to DIOTs with the same milling time. The possible reasons are highlighted in the subsequent paragraphs.

Tab. 1 shows that the basicity R = CaO/SiO_2 of RIOTs was only 0.08, indicating that the RIOTs used in the study had very low pozzolanic reactivity [41]. However, the binding energy of Si2p, Al2p, and O1s decreased after 60 min of wet grinding (Fig. 10), indicating a certain degree of increase in pozzolanic activity. Nonetheless, the surface binding energy of DIOTs was lower than that of WIOTs under the same grinding time, suggesting that wet grinding had no advantage in stimulating the pozzolanic reactivity of IOTs compared to dry grinding. Therefore, the higher activity index of WIOTs was not due to an increase in pozzolanic activity. In fact, particle characteristics are the most important factors affecting the activity of the mineral admixture with low pozzolanic reactivity. According to Han et al. [4], increasing the fineness of IOTs enhances a finer pore structure and higher compressive strength of the mortar containing IOTs. Fig. 2 highlights that WIOTs had finer particles compared to DIOTs. Therefore, the presence of a large number of fine particles in WIOTs could increase the compactness of cement mortar, and this was beneficial in improving the mechanical properties of the cement-based material. Moreover, the specific surface area of WIOTs60 was almost two times higher than that of DIOTs60 (Fig. 2b). This larger specific surface area of WIOTs60 could provide a broader contact area with NaOH solution and promote ion dissolution (Fig. 4).

In addition, supplementary cementitious materials such as slag, fly ash, and limestone can act as nucleation seeds to induce the hydration of cement. Notably, the smaller the particles, the greater the ability to induce nucleation [42]. In order to study the nucleation effect of IOTs, The DIOTs60 and WIOTs60 were mixed with cement at a proportion of 1:1, respectively. The pastes were prepared with a water/solids ratio of 0.5. After 4 h of hydration, the pastes were relatively young and not set at that time. After dehydration and vacuum drying, the pastes collapsed into powder, and the surface of IOTs60 particles was distinguished through SEM. Results are shown in Fig. 12. It was found that the surface characteristic of DIOTs60 particles was similar to that of WIOTs60 particles. In addition, numerous products of hydration were observed on the surfaces of both DIOTs60 and WIOTs60 particles. Hexagonal bar like particles, hexagonal plate particles, and “sea anemone” type particles are considered

to be ettringite, calcium hydroxide, and C-S-H, respectively [42]. These observations confirmed that the surface of IOTs could also act as a substrate for the nucleation of the hydrates. In addition, Fig. 2a shows that the d (0.1) value of WIOTs60 was 976 nm, indicating that almost 10% of the particles had a micro size of around 900 nm. These tiny particles could induce nucleation in the cement hydration process and promote the hydration of cement, thus improving the strength of the cement mortar containing WIOTs60.

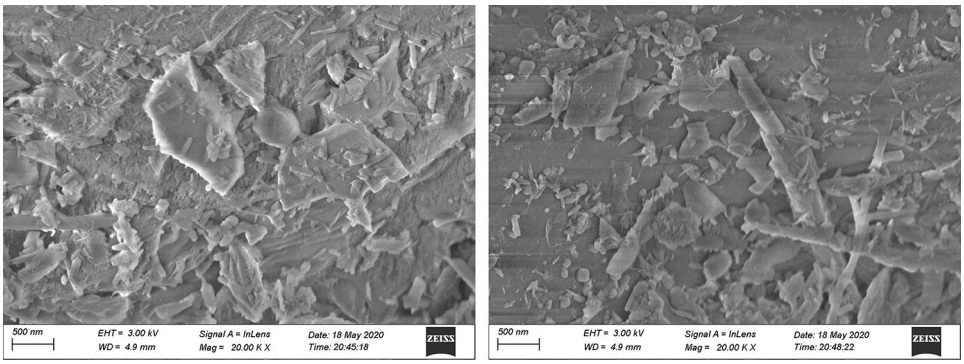

(a) (b)

Figure 12: DIOTs (on the left) and WIOTs surface (on the right), respectively (a) and (b) after 4 h

Based on the analysis, the wet-milling technique may be developed for IOTs resource utilization in building materials, owing to its excellent economic, technological, and environmental benefits. Firstly, compared to dry grinding, wet grinding reduced the particle size of IOTs and stimulated their activity more efficiently. The finer the iron tailings powder is, the larger the replacement limit in sustainable building materials can be obtained. Using WIOTs as supplementary cementitious materials to partially replace cement is not only an effective way to utilize solid waste but also can save cement and reduce carbon dioxide emissions. Secondly, most IOTs are directly discharged into the river or exposed to rainwater and can be ground by adding a proper amount of water directly, while the dry grinding process usually requires the powder to be pre-dried. The omission of the pre-drying process also helps save energy. Due to the presence of water, the generation of dust can be avoided when wet grinding IOTs during the production process, thereby reducing the pollution of the production environment. In addition, it is worth noting that the WIOTs output is in a slurry state, which can be directly utilized in the concrete mixture without drying. As we know, the dispersion of mineral admixture has an important influence on the microstructure of cement-based materials. The slurry prepared by wet grinding is easier to disperse evenly than dry powder, which helps cement-based materials to form a denser and uniform microstructure. Therefore, substantial economic and environmental benefits can be obtained.

5 Conclusions

From the discussion, it can be concluded that:

(1) Compared to the traditional milling method, wet grinding showed higher efficiency in generating finer particles. IOTs with d (0.5) of 6.203 μm, which were extremely difficult to obtain by dry-grinding, could be generated with ease using the wet grinding system.

(2) The dissolution of silicon and aluminum ions from alkaline solutions could significantly be facilitated by wet-grinding, and the reactivity index of WIOTs was higher than that of DIOTs under the same milling time. This indicated that wet grinding was more efficient in inducing the activity of IOTs than dry grinding.

(3) Wet grinding could significantly decrease the crystallinity of quartz and damage the crystal structure of IOTs. Additionally, more lattice distortion and defects were produced in the physical structure of WIOTs.

(4) To a certain extent, both dry and wet grinding could destroy the stability of Si-O bonds and decrease the surface binding energy under a long duration of grinding.

(5) WIOTs, had more micro particles, could offer more nuclei sites for the cement hydrates, and exhibited a greater ability to induce nucleation.

(6) The findings uncovered a new process of disposing of IOTs and proposed a novel method of utilizing IOTs in cement-based materials.

Acknowledgement: We gratefully acknowledge the anonymous reviewers for their careful work and thoughtful suggestions that have helped improve this paper substantially.

Funding Statement: This work was supported by University Natural Science Research Project of Anhui Province (KJ2019A0171).

Conflicts of Interest: The authors declare that they have no conflicts of interest to report regarding the present study.

References

1. Cheng, Y. H., Huang, F., Li, W. C., Liu, R., Li, G. L. et al. (2016). Test research on the effects of mechanochemically activated iron tailings on the compressive strength of concrete. *Construction and Building Materials, 118(5),* 164–170. DOI 10.1016/j.conbuildmat.2016.05.020.
2. Luo, L., Zhang, Y. M., Bao, S. X., Chen, T. J. (2016). Utilization of iron ore tailings as raw material for Portland cement clinker production. *Advances in Materials Science and Engineering, 2016,* 1–6. DOI 10.1155/2016/1596047.
3. Zhou, M. K., Zhu, Z. G., Li, B. X., Liu, J. C. (2017). Volcanic activity and thermal excitation of rich-silicon iron ore tailing in concrete. *Journal of Wuhan University of Technology-Materials Science Edition, 32(2),* 365–372. DOI 10.1007/s11595-017-1604-z.
4. Han, F. H., Li, L., Song, S. M., Liu, J. H. (2017). Early-age hydration characteristics of composite binder containing iron tailing powder. *Powder Technology, 315,* 322–331. DOI 10.1016/j.powtec.2017.04.022.
5. Carrasco, E. V. M., Magalhaes, M. D. C., Santos, W. J. D., Alves, R. C., Mantilla, J. N. R. (2017). Characterization of mortars with iron ore tailings using destructive and nondestructive tests. *Construction and Building Materials, 131(2),* 31–38. DOI 10.1016/j.conbuildmat.2016.11.065.
6. Li, C., Sun, H. H., Bai, J., Li, L. T. (2010). Innovative methodology for comprehensive utilization of iron ore tailings Part 1. The recovery of iron from iron ore tailings using magnetic separation after magnetizing roasting. *Journal of Hazardous Materials, 174(1–3),* 71–77. DOI 10.1016/j.jhazmat.2009.09.018.
7. Fontes, W. C., Mendes, J. C., Da Silva, S. N., Peixoto, R. A. F. (2016). Mortars for laying and coating produced with iron ore tailings from tailing dams. *Construction and Building Materials, 112(4),* 988–995. DOI 10.1016/j.conbuildmat.2016.03.027.
8. Li, C., Sun, H. H., Yi, Z. L., Li, L. T. (2010). Innovative methodology for comprehensive utilization of iron ore tailings Part 2: The residues after iron recovery from iron ore tailings to prepare cementitious material. *Journal of Hazardous Materials, 174(1–3),* 78–83. DOI 10.1016/j.jhazmat.2009.09.019.
9. Young, G., Yang, M. (2019). Preparation and characterization of Portland cement clinker from iron ore tailings. *Construction and Building Materials, 197(1),* 152–156. DOI 10.1016/j.conbuildmat.2018.11.236.
10. Zhao, S. J., Fan, J. J., Sun, W. (2014). Utilization of iron ore tailings as fine aggregate in ultra-high performance concrete. *Construction and Building Materials, 50(10),* 540–548. DOI 10.1016/j.conbuildmat.2013.10.019.
11. Huang, X. Y., Ranade, R., Ni, W., Li, V. C. (2013). Development of green engineered cementitious composites using iron ore tailings as aggregates. *Construction and Building Materials, 44(5),* 757–764. DOI 10.1016/j.conbuildmat.2013.03.088.

12. Shettima, A. U., Hussin, M. W., Ahmad, Y., Mirza, J. (2016). Evaluation of iron ore tailings as replacement for fine aggregate in concrete. *Construction and Building Materials, 120(1–3),* 72–79. DOI 10.1016/j.conbuildmat.2016.05.095.
13. Cui, X. W., Wang, C. L., Ni, W., Di, Y. Q., Cui, H. L. et al. (2017). Study on the reaction mechanism of autoclaved aerated concrete based on iron ore tailings. *Revista Romana De Materiale–Romanian Journal of Materials, 47(1),* 46–53.
14. Liang, X. Y., Yuan, D. X., Li, J., Wang, C. L., Lin, X. R. et al. (2018). Preparation and phase characteristics of autoclaved aerated concrete using iron ore tailings. *Revista Romana De Materiale–Romanian Journal of Materials, 48(3),* 381–387.
15. Wang, C. L., Ni, W., Zhang, S. Q., Wang, S., Gai, G. S. et al. (2016). Preparation and properties of autoclaved aerated concrete using coal gangue and iron ore tailings. *Construction and Building Materials, 104,* 109–115. DOI 10.1016/j.conbuildmat.2015.12.041.
16. Yao, R., Liao, S. Y., Dai, C. L., Liu, Y. C., Chen, X. Y. et al. (2015). Preparation and characterization of novel glass-ceramic tile with microwave absorption properties from iron ore tailings. *Journal of Magnetism and Magnetic Materials, 378,* 367–375. DOI 10.1016/j.jmmm.2014.11.066.
17. Fontes, W. C., de Carvalho, J. M. F., Andrade, L. C. R., Segadaes, A. M., Peixoto, R. A. F. (2019). Assessment of the use potential of iron ore tailings in the manufacture of ceramic tiles: From tailings-dams to "brown porcelain". *Construction and Building Materials, 206,* 111–121. DOI 10.1016/j.conbuildmat.2019.02.052.
18. Das, S. K., Kumar, S., Ramachandrarao, P. (2000). Exploitation of iron ore tailing for the development of ceramic tiles. *Waste Management, 20(8),* 725–729. DOI 10.1016/S0956-053X(00)00034-9.
19. Li, W. S., Lei, G. Y., Xu, Y., Huang, Q. F. (2018). The properties and formation mechanisms of eco-friendly brick building materials fabricated from low-silicon iron ore tailings. *Journal of Cleaner Production, 204,* 685–692. DOI 10.1016/j.jclepro.2018.08.309.
20. Yang, C. M., Cui, C., Qin, J., Cui, X. Y. (2014). Characteristics of the fired bricks with low-silicon iron tailings. *Construction and Building Materials, 70(4),* 36–42. DOI 10.1016/j.conbuildmat.2014.07.075.
21. Mendes, B. C., Pedroti, L. G., Fontes, M. P. F., Ribeiro, J. C. L., Vieira, C. M. F. et al. (2019). Technical and environmental assessment of the incorporation of iron ore tailings in construction clay bricks. *Construction and Building Materials, 227,* 116669. DOI 10.1016/j.conbuildmat.2019.08.050.
22. Luo, L. Q., Li, K. Y., Fu, W., Liu, C., Yang, S. Y. (2020). Preparation, characteristics and mechanisms of the composite sintered bricks produced from shale, sewage sludge, coal gangue powder and iron ore tailings. *Construction and Building Materials, 232(1–3),* 117250. DOI 10.1016/j.conbuildmat.2019.117250.
23. Yao, G., Wang, Q., Wang, Z. M., Wang, J. X., Lyu, X. J. (2020). Activation of hydration properties of iron ore tailings and their application as supplementary cementitious materials in cement. *Powder Technology, 360,* 863–871. DOI 10.1016/j.powtec.2019.11.002.
24. Tang, C., Li, K. Q., Ni, W., Fan, D. C. (2019). Recovering iron from iron ore tailings and preparing concrete composite admixtures. *Minerals, 9(4),* 232. DOI 10.3390/min9040232.
25. Huang, X. Y., Ranade, R., Li, V. C. (2013). Feasibility study of developing green ECC using iron ore tailings powder as cement replacement. *Journal of Materials in Civil Engineering, 25(7),* 923–931. DOI 10.1061/(ASCE)MT.1943-5533.0000674.
26. Cheng, Y. H., Huang, F., Li, W. C., Liu, R., Li, G. L. et al. (2016). Test research on the effects of mechanochemically activated iron tailings on the compressive strength of concrete. *Construction and Building Materials, 118(5),* 164–170. DOI 10.1016/j.conbuildmat.2016.05.020.
27. Yao, G., Wang, Q., Su, Y. W., Wang, J. X., Qiu, J. et al. (2020). Mechanical activation as an innovative approach for the preparation of pozzolan from iron ore tailings. *Minerals Engineering, 145,* 106068. DOI 10.1016/j.mineng.2019.106068.
28. Piao, C., Wang, D., Zhang, L., Wang, C., Liu, H. (2016). Influence of chemical mechanical coupling effect on iron ore tailings cementitious activity. *Journal of Basic Science and Engineering, 24(6),* 1100–1109. DOI 10.16058/j.issn.1005-0930.2016.06.003 (in Chinese).
29. Zheng, Y. C., Li, Q., Liu, Y. J. (2013). Mine tailing as alternative to clay for producing belite cement clinker. *Advanced Materials Research, 726,* 2704–2713. DOI 10.4028/www.scientific.net/AMR.726-731.2704.

30. Duan, P., Yan, C. J., Zhou, W., Ren, D. M. (2016). Fresh properties, compressive strength and microstructure of fly ash geopolymer paste blended with iron ore tailing under thermal cycle. *Construction and Building Materials, 118(16),* 76–88. DOI 10.1016/j.conbuildmat.2016.05.059.
31. Mitrovic, A., Zdujic, M. (2014). Preparation of pozzolanic addition by mechanical treatment of kaolin clay. *International Journal of Mineral Processing, 132,* 59–66. DOI 10.1016/j.minpro.2014.09.004.
32. Boldyrev, V. V. (2006). Mechanochemistry and mechanical activation of solids. *ChemInform, 37(31),* 177. DOI 10.1002/chin.200631230.
33. Yang, J., Huang, J. X., Su, Y., He, X. Y., Tan, H. B. et al. (2019). Eco-friendly treatment of low-calcium coal fly ash for high pozzolanic reactivity: A step towards waste utilization in sustainable building material. *Journal of Cleaner Production, 238(1),* 117962. DOI 10.1016/j.jclepro.2019.117962.
34. Kumar, S., Mucsi, G., Kristaly, F., Pekker, P. (2017). Mechanical activation of fly ash and its influence on micro and nano-structural behaviour of resulting geopolymers. *Advanced Powder Technology, 28(3),* 805–813. DOI 10.1016/j.apt.2016.11.027.
35. Tan, H. B., Zhang, X., He, X. Y., Guo, Y. L., Deng, X. F. et al. (2018). Utilization of lithium slag by wet-grinding process to improve the early strength of sulphoaluminate cement paste. *Journal of Cleaner Production, 205(10),* 536–551. DOI 10.1016/j.jclepro.2018.09.027.
36. Wang, Y. B., He, X. Y., Su, Y., Tan, H. B., Yang, J. et al. (2018). Self-hydration characteristics of ground granulated blast-furnace slag (GGBFS) by wet-grinding treatment. *Construction and Building Materials, 167,* 96–105. DOI 10.1016/j.conbuildmat.2018.01.178.
37. Kotake, N., Kuboki, M., Kiya, S., Kanda, Y. (2011). Influence of dry and wet grinding conditions on fineness and shape of particle size distribution of product in a ball mill. *Advanced Powder Technology, 22(1),* 86–92. DOI 10.1016/j.apt.2010.03.015.
38. Guzzo, P. L., de Barros, F. B. M., Tino, A. A. D. (2019). Effect of prolonged dry grinding on size distribution, crystal structure and thermal decomposition of ultrafine particles of dolostone. *Powder Technology, 342,* 141–148. DOI 10.1016/j.powtec.2018.09.064.
39. Bu, X. N., Chen, Y. R., Ma, G. X., Sun, Y. J., Ni, C. et al. (2019). Differences in dry and wet grinding with a high solid concentration of coking coal using a laboratory conical ball mill: Breakage rate, morphological characterization, and induction time. *Advanced Powder Technology, 30(11),* 2703–2711. DOI 10.1016/j.apt.2019.08.016.
40. Guo, W., Li, D. X., Chen, J. H., Yang, N. R. (2007). Rapid evaluation method of the pozzolanic reactive activity of coal gangue. *Journal of the Chinese Ceramic Society, 35(4),* 489–494. DOI 10.1016/S1001-6058(07)60030-4 (in Chinese).
41. Sharonova, O. M., Solovyov, L. A., Oreshkina, N. A., Yumashev, V. V., Anshits, A. G. (2010). Composition of high-calcium fly ash middlings selectively sampled from ash collection facility and prospect of their utilization as component of cementing materials. *Fuel Processing Technology, 91(6),* 573–581. DOI 10.1016/j.fuproc.2010.01.003.
42. Berodier, E., Scrivener, K. (2014). Understanding the filler effect on the nucleation and growth of C-S-H. *Journal of the American Ceramic Society, 97(12),* 3764–3773. DOI 10.1111/jace.13177.